Electronic Supplementary Material (ESI) for ChemComm.

Supplementary Information

Convergent heteroditopic cyclo[6]aramides as macrocyclic ion-pair receptors for constructing [2]pseudorotaxanes

Jinchuan Hu,[a] Long Chen,[a] Jie Shen,[b] Jian Luo,[a] Pengchi Deng,[a] Yi Ren,[a] Huaqiang Zeng,[b] Wen Feng*[a] and Lihua Yuan*[a]

[a] *Key Laboratory for Radiation Physics and Technology of Ministry of Education, Institute of Nuclear Science and Technology, College of Chemistry, Analytical & Testing Center, Sichuan University, Chengdu, 610064, China.*

[b] *Institute of Bioengineering and Nanotechnology, 31 Biopolis Way, The Nanos, 138669, Singapore*

E-mail: lhyuan@scu.edu.cn; wfeng9510@scu.edu.cn

Fax: +86 28 85418755

Contents

1. Materials and methods

The ^{1}H NMR and ^{13}C NMR spectra were recorded on Bruker AVANCE AV II-400 MHz (^{1}H: 400 MHz; ^{13}C: 100 MHz). $CDCl_3$, CD_3COCD_3, CD_3CN and DMSO-d_6 were purchased from Cambridge Isotope Laboratories, used for the titration experiments without further drying. Chemical shifts are reported in δ values in ppm using tetramethylsilane (TMS) and coupling constants (J) are denoted in Hz. Multiplicities are denoted as follows: s = singlet, d = doublet, t = triplet, dd = double doublet and m = multiplet. High resolution mass (HRMS) data were collected by WATERS Q-TOF Premier. All chemicals were obtained from commercial suppliers and were used as received unless other-wise noted. CH_2Cl_2 was dried over CaH_2. Column chromatography was carried out using silica gel (300-400 mesh). Solvents for extraction and chromatography were reagent grade. Crystallographic studies were performed on compounds **2b** and [2] pseudorotaxane **2b ⊂G1**. Data were collected on a Xcalibur E diffractometer with graphite monochromated Mo-Kα radiation (λ = 0.7107 Å).

2. Synthesis

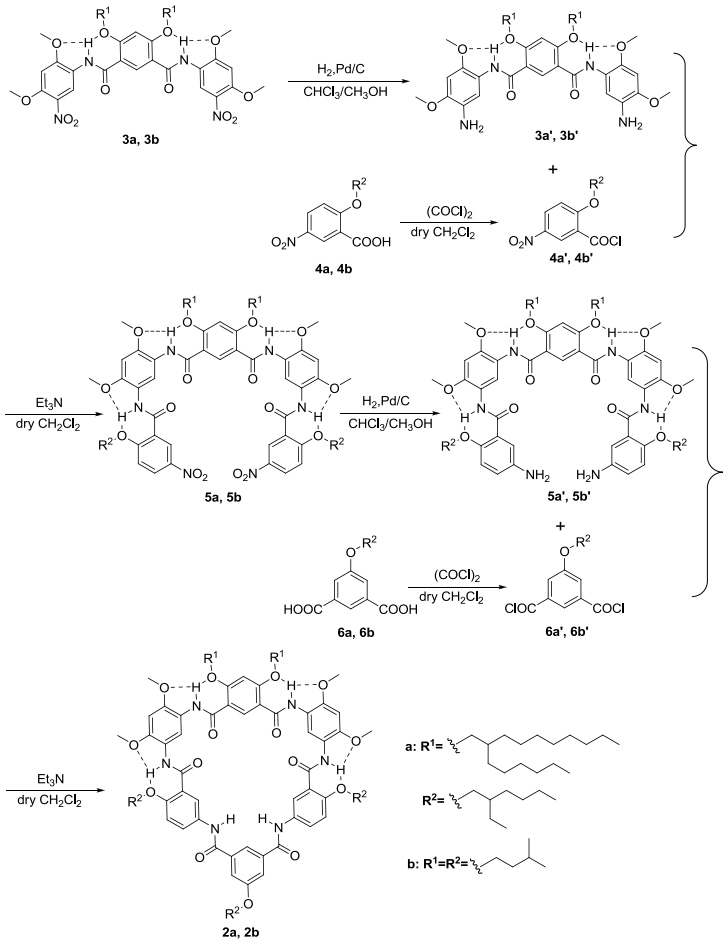

Scheme S1. Synthetic routes for macrocycles **2**.

Compounds **3a**, **3b**, **5a** and **5b** were converted into **3a'**, **3b'**, **5a'** and **5b'** by catalytic hydrogenation, respectively. Compounds **3a'**, **3b'**, **5a'** and **5b'** were used directly in the subsequent reaction without further purification.

Compounds **3a**,[1] **3b**,[1] **4a**,[2] **4b**,[2] **6a**[3] and **6b**[3] were synthesized according to analogous literature procedures.

Compound **3a**: A yellow solid; ^{1}H NMR (400 MHz, $CDCl_3$, 298 K): δ= 9.73 (s, 2H), 9.20 (s, 2H), 8.86 (s, 1H), 6.41 (s, 3H), 4.12 (d, *J*=6.0 Hz, 4H), 4.05 (s, 6H), 3.83 (s, 6H), 2.01 (m, 2H), 1.45-1.24 (m, 48H), 0.85 (m, 12H); ^{13}C NMR (100 MHz, $CDCl_3$, 298 K): δ 161.86, 160.26, 153.59, 150.95, 137.26, 131.27, 121.05, 118.41, 114.51, 96.40, 95.43, 73.23, 56.58, 56.45, 37.59, 31.88, 31.79, 31.03, 30.09, 29.72, 29.57, 29.33, 26.60, 22.64, 14.06; ESI-HRMS (m/z) calcd for $C_{56}H_{86}N_4O_{12}$ $[M+H]^+$ 1007.6320, $[M+Na]^+$ 1029.6140, found $[M+H]^+$ 1007.6320, $[M+Na]^+$ 1029.6033.

Compound **5a**: Trimer **3a** (500 mg, 0.50 mmol) was hydrogenated in the presence of 20% Pd/C (100 mg) in $CHCl_3/CH_3OH$ (60 mL, v/v=5:1) for 10 h at 40 ℃. The

solution was filtered in darkness as fast as possible followed by immediate removal of the solvent. The reduced diamine was used for the immediate coupling reaction. DMF (5 uL) was added to a suspension of compound **4a** (416 mg, 1.02 mmol) and oxalyl chloride (388 mg, 3.06 mmol) in CH_2Cl_2. The mixture was stirred for 40 min at room temperature. The solvent was evaporated and the resulting acid chloride was dried in vacuum at room temperature for 30 min to get compound **4a'**. Compound **4a'** was dissolved in CH_2Cl_2 (60 mL) and added dropwise to a mixture of the above **3a'** and Et_3N (200 mg, 1.98 mmol) in CH_2Cl_2 (20 mL) at room temperature. The solution was stirred under N_2 for 7 h. The organic layer was washed with water (20 mL×3) and dried over anhydrous Na_2SO_4. Concentration under reduced pressure afforded a yellow solid which was triturated with ethyl acetate and filtered to give pentamer **5a** (626 mg, 83.4%) as a yellow solid. ^{1}H NMR (400 MHz, $CDCl_3$, 298 K): δ = 9.63 (s, 2H), 9.57 (s, 2H), 9.25 (s, 2H), 9.21 (s, 1H), 9.18 (d, *J* = 2.8 Hz, 2H), 8.21 (q, J_1 = 2.8 Hz, J_2 = 9.2 Hz, 2H), 7.09 (d, *J* = 9.2 Hz, 2H), 6.54 (s, 1H), 6.48 (s, 2H), 4.21 (d, *J* = 5.6 Hz, 4H), 4.12 (d, *J*=6.2 Hz, 4H), 3.87 (s, 12H), 1.98 (m, 4H), 1.53-1.22 (m, 64H), 0.94-0.84 (m, 24H); ^{13}C NMR (100 MHz, $CDCl_3$, 298 K): δ 162.09, 161.28, 160.51, 160.10, 146.93, 146.51, 141.58, 128.74, 127.73, 123.22, 120.67, 119.59, 117.46, 115.86, 112.70, 96.59, 74.81, 73.30, 72.83, 55.85, 38.61, 37.67, 31.79, 31.08, 30.00, 29.67, 29.59, 29.32, 28.76, 26.71, 23.45, 22.95, 22.64, 14.08, 13.99, 10.62; ESI-HRMS (m/z) calcd for $C_{86}H_{128}N_6O_{16}$ $[M+H]^+$ 1501.9465, $[M+Na]^+$ 1523.9285, found $[M+H]^+$ 1501.9465, $[M+Na]^+$ 1523.9282.

Compound **2a**: Pentamer **5a** (400 mg, 0.27 mmol) was hydrogenated in the presence of 20% Pd/C (80 mg) in $CHCl_3$/CH_3OH (100 mL, v/v = 5:1) for 10 h at 40 ℃. The solution was filtered in darkness as fast as possible followed by immediate removal of the solvent. The reduced diamine was used for the immediate coupling reaction. DMF (5 uL) was added to a suspension of compound **6a** (82 mg, 0.28 mmol) and oxalyl chloride (105 mg, 0.84 mmol) in CH_2Cl_2. The mixture was stirred for 40 min at room temperature. The solvent was evaporated and the resulting acid chloride was dried in vacuum at room temperature for 30 min to get compound **6a'**. Compound **6a'** was dissolved in CH_2Cl_2 (60 mL) and added dropwise to a mixture of the above **5a'** and Et_3N (162 mg, 1.60 mmol) in CH_2Cl_2 (20 mL) at 0 ℃. The solution was stirred under N_2 for 7 h. The organic layer was washed with water (20 mL × 3) and dried over anhydrous Na_2SO_4 and filtered. The crude product was purified by chromatography on silica gel (CH_2Cl_2/MeOH = 20: 1) to provide the product **2a** as a white solid (339 mg, 74.6%). ^{1}H NMR (400 MHz, $CDCl_3$, 298 K): δ = 10.20 (s, 2H), 9.42 (s, 2H), 9.39 (s, 2H), 9.16 (s, 2H), 9.15 (s, 1H), 8.51 (d, *J* = 6.2 Hz, 2H), 8.23 (s, 1H), 8.19 (s, 2H), 7.75 (s, 2H), 7.01 (d, *J* = 6.2 Hz, 2H), 6.50 (s, 2H), 6.49 (s, 1H), 4.06 (m, 10H), 3.89 (s, 6H), 3.88 (s, 6H), 2.00 (m, 4H), 1.77 (m, 1H), 1.53-1.26 (m, 72H), 0.92-0.85 (m, 30H); ^{13}C NMR (100 MHz, $CDCl_3$, 298 K): δ 164.86, 163.45, 162.54, 159.98, 159.73, 153.26, 145.94, 135.55, 132.77, 125.17, 123.74, 121.86, 120.80, 119.48, 118.02, 117.61, 112.68, 94.73, 72.51, 55.92, 55.51, 39.37, 38.66, 37.81, 31.89, 30.91, 30.45, 30.03, 29.90, 29.72, 29.59, 29.34, 29.08, 28.74, 26.63, 23.80, 23.29, 23.07, 22.64, 14.10, 11.13, 10.41. ESI-HRMS (m/z) calcd for $C_{102}H_{150}N_6O_{15}$ $[M+Na]^+$ 1723.1090,

found $[M+Na]^+$ 1723.1082.

Compound **2b**: Prepared according to the same method as for **2a**. ^{1}H NMR (400 MHz, $CDCl_3$, 298 K, containing 1.5 equiv Et_2NH_2Cl): δ=10.80 (s, 2H), 10.50 (s, 2H), 9.76 (s, 2H), 9.35 (s, 2H), 9.26 (s, 1H), 8.99 (s, 1H), 8.72 (d, *J*=9.2 Hz, 2H), 8.63 (s, 2H), 7.80 (s, 2H), 7.05 (d, *J*=9.2 Hz, 2H), 6.57 (s, 2H), 6.53 (s, 1H), 4.26 (m, 8H), 4.11 (t, *J*=6.3 Hz, 2H), 3.94 (s, 12H), 1.97 (m, 8H), 1.89 (m, 2H), 1.71 (m, 5H), 1.07 (d, *J*=5.1 Hz, 12H), 1.01 (d, *J*=5.6 Hz, 12H), 0.96 (d, *J*=6.4 Hz, 6H); ^{13}C NMR (100 MHz, $CDCl_3$ + 40% CD_3OD, 298 K): δ 166.69, 166.08, 163.96, 163.15, 156.55, 148.75, 142.95, 142.35, 138.30, 136.18, 135.06, 132.62, 127.74, 123.60, 122.57, 117.09, 115.08, 96.93, 72.31, 58.84, 42.08, 41.69, 41.19, 35.78, 33.45, 33.15, 29.15, 26.60, 26.38, 17.64, 14.57; ESI-HRMS (m/z) calcd for $C_{71}H_{88}N_6O_{15}$ $[M+H]^+$ 1265.6386, found $[M+H]^+$ 1265.6390.

3. ^{1}H NMR and ^{13}C NMR spectra of new compounds

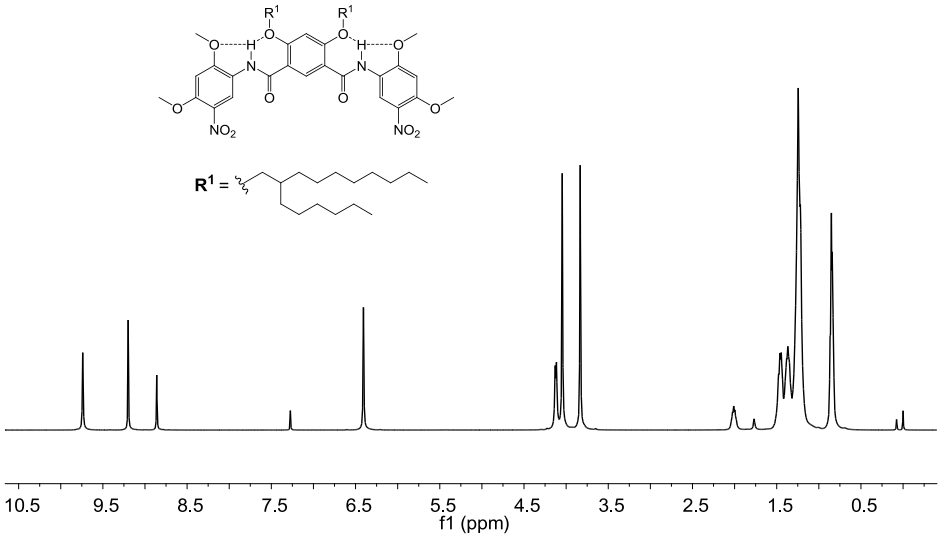

Figure S1. ^{1}H NMR spectrum of **3a** (400 MHz, $CDCl_3$, 298 K).

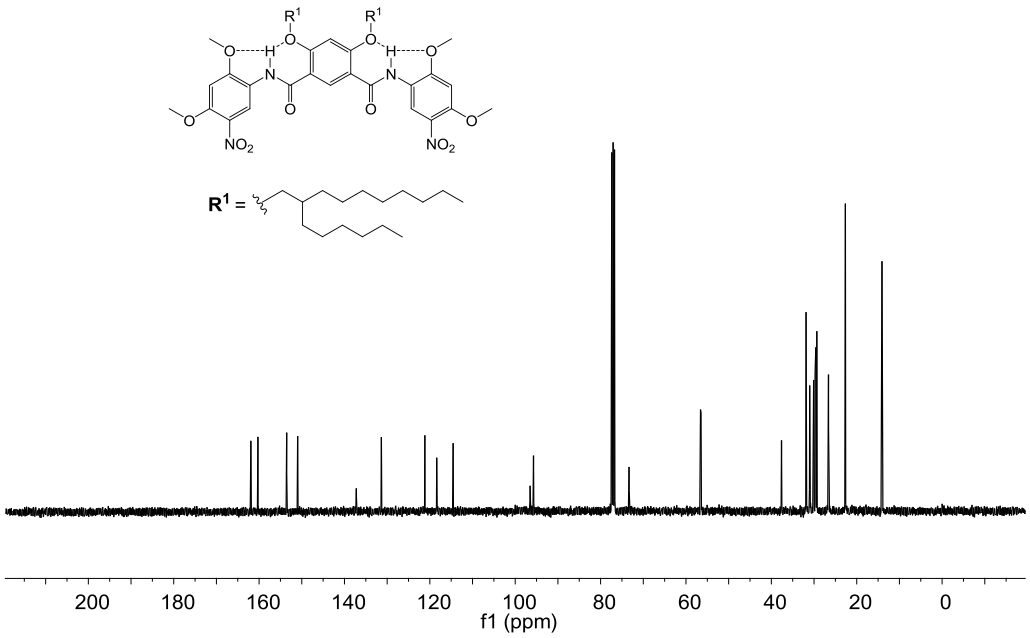

Figure S2. ^{13}C NMR spectrum of **3a** (100 MHz, $CDCl_3$, 298 K).

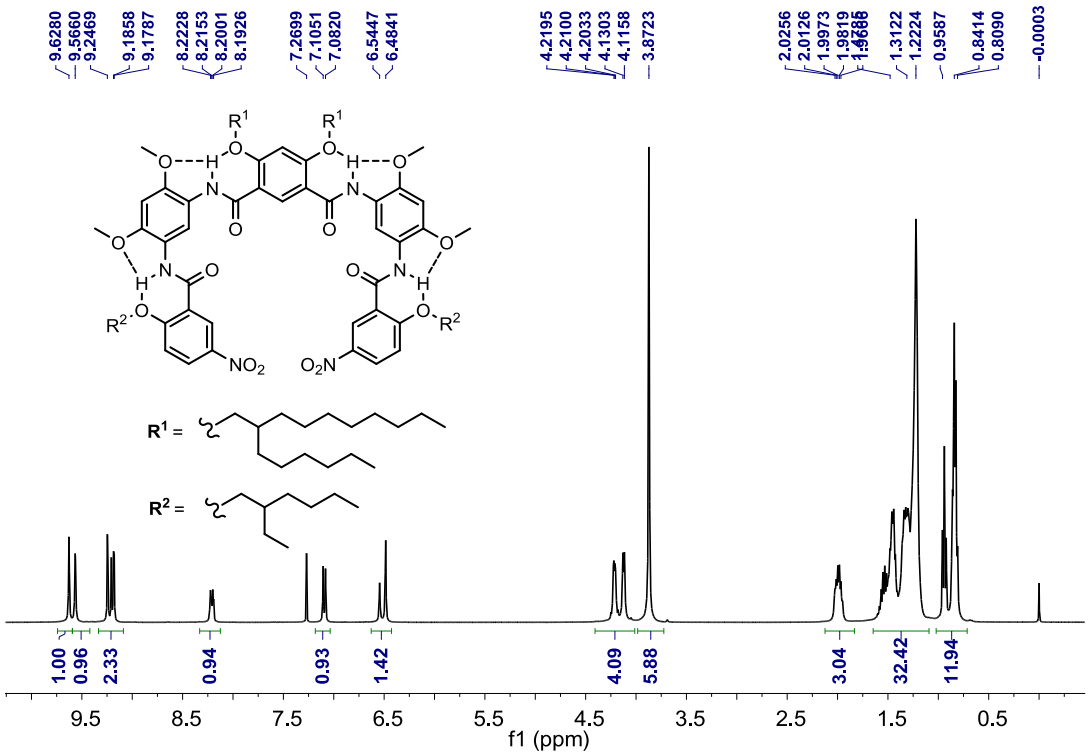

Figure S3. ^{1}H NMR spectrum of **5a** (400 MHz, $CDCl_3$, 298 K).

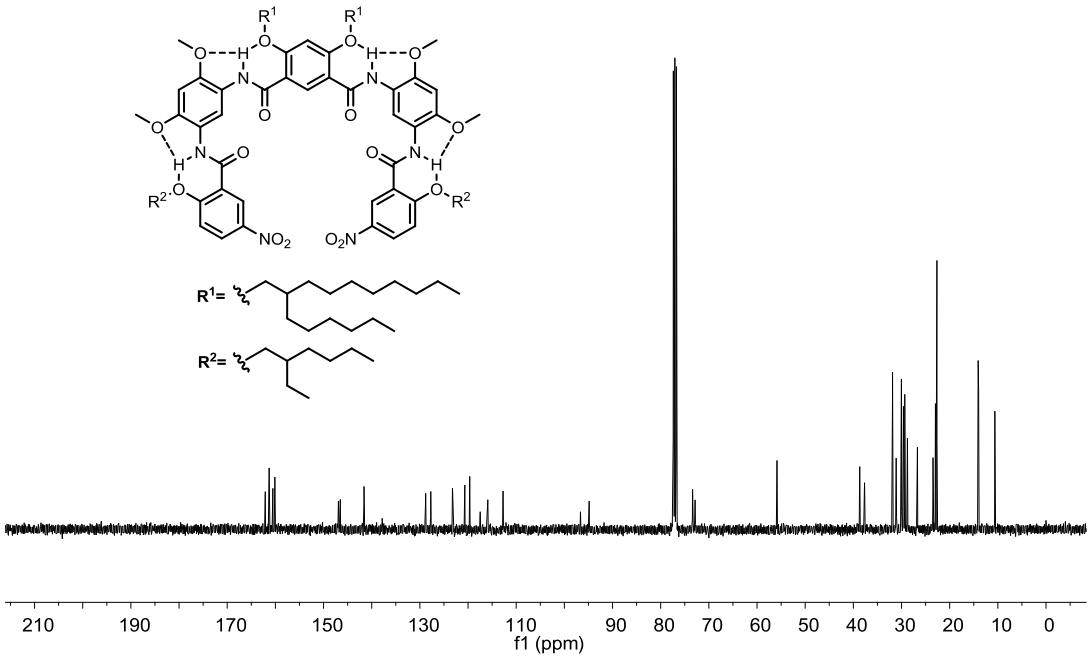

Figure S4. ^{13}C NMR spectrum of **5a** (100 MHz, $CDCl_3$, 298 K).

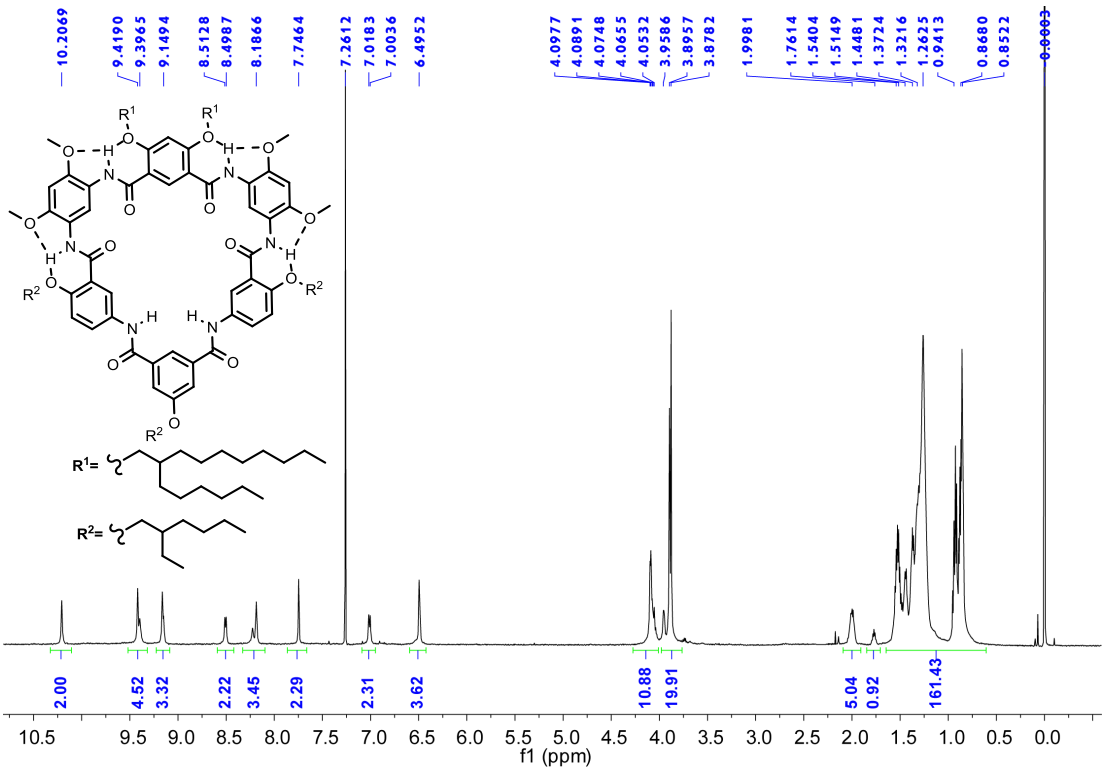

Figure S5. ^{1}H NMR spectrum of **2a** (400 MHz, $CDCl_3$, 298 K).

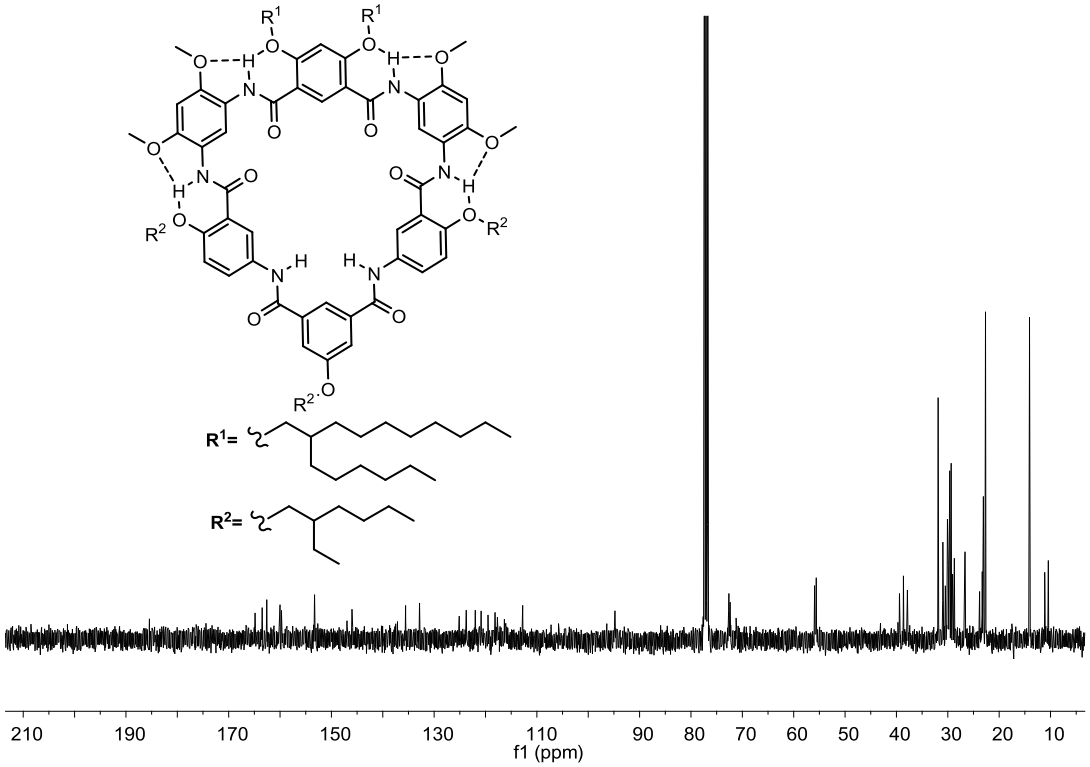

Figure S6. ^{13}C NMR spectrum of **2a** (100 MHz, $CDCl_3$, 298 K).

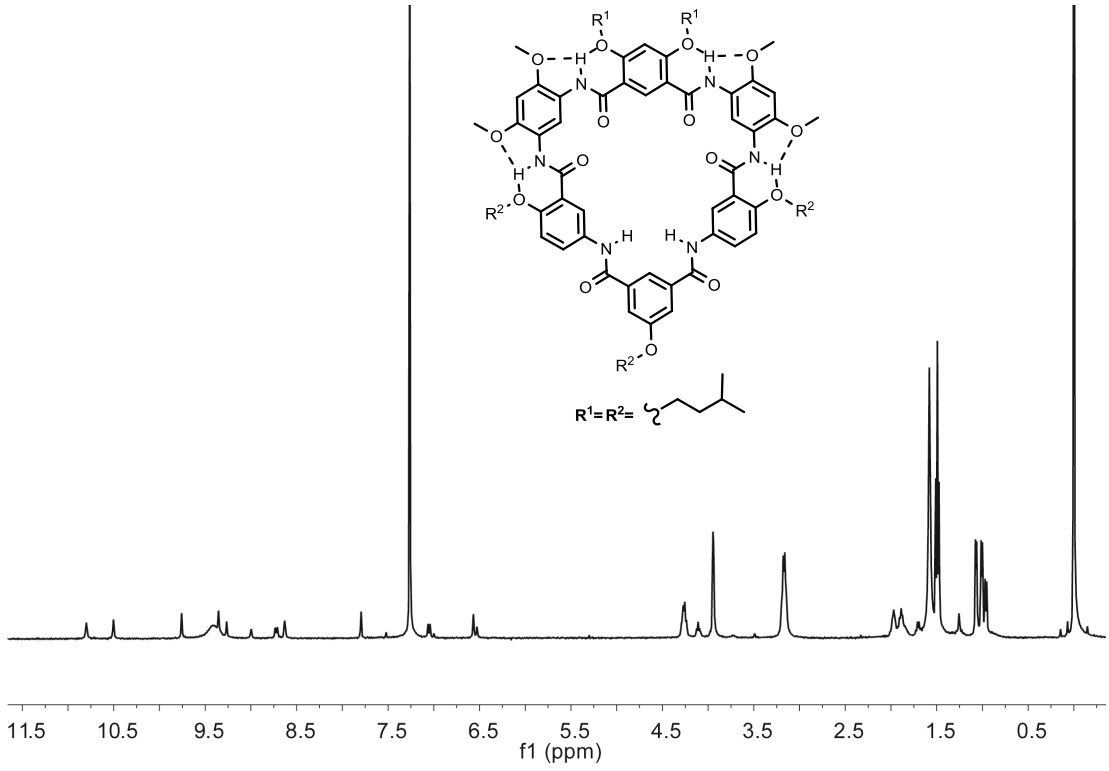

Figure S7. ^{1}H NMR spectrum of **2b** (400 MHz, $CDCl_3$, 298 K, containing 1.5 equiv Et_2NH_2Cl).

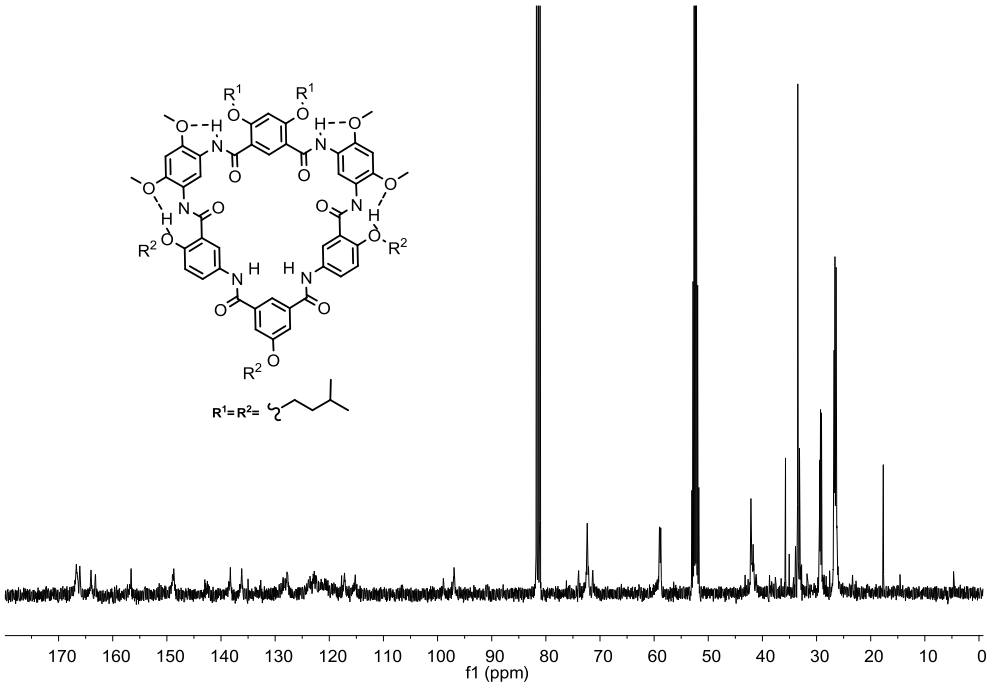

Figure S8. ^{13}C NMR spectrum of **2b** (100 MHz, $CDCl_3$+40% CD_3OD, 298 K).

4. Concentration-dependent ^1H NMR spectra of **2a**

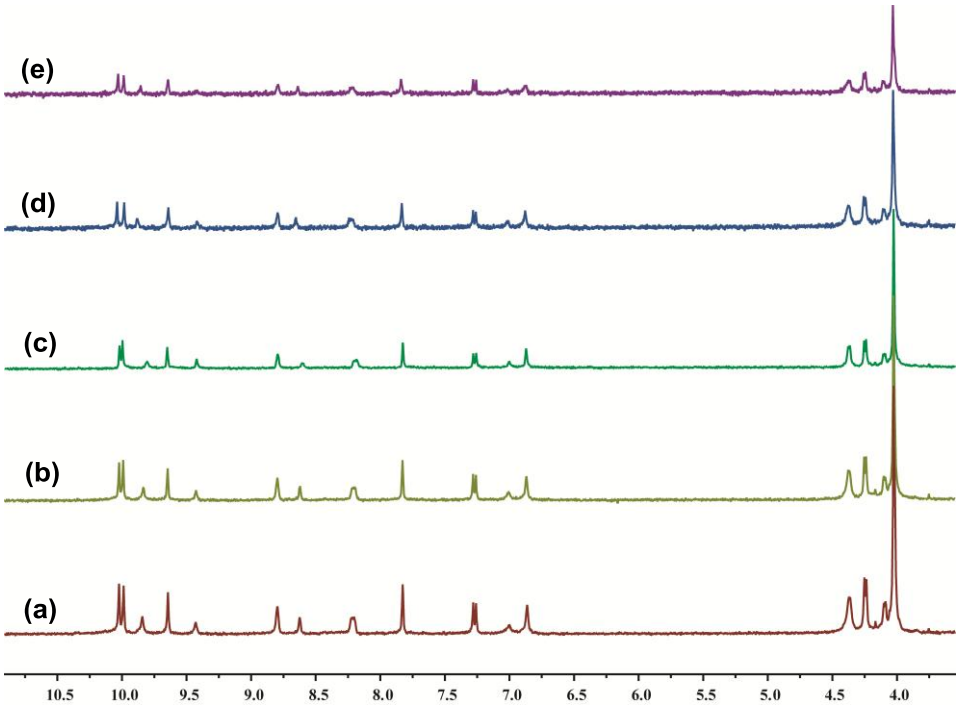

Figure S9. Stacked partial ^1H NMR spectra (400 MHz, acetone-d_6, 298 K) of **2a** at 1.5 mM (a), 1.0 mM (b), 0.7 mM (c), 0.5 mM (d) and 0.3 mM (e).

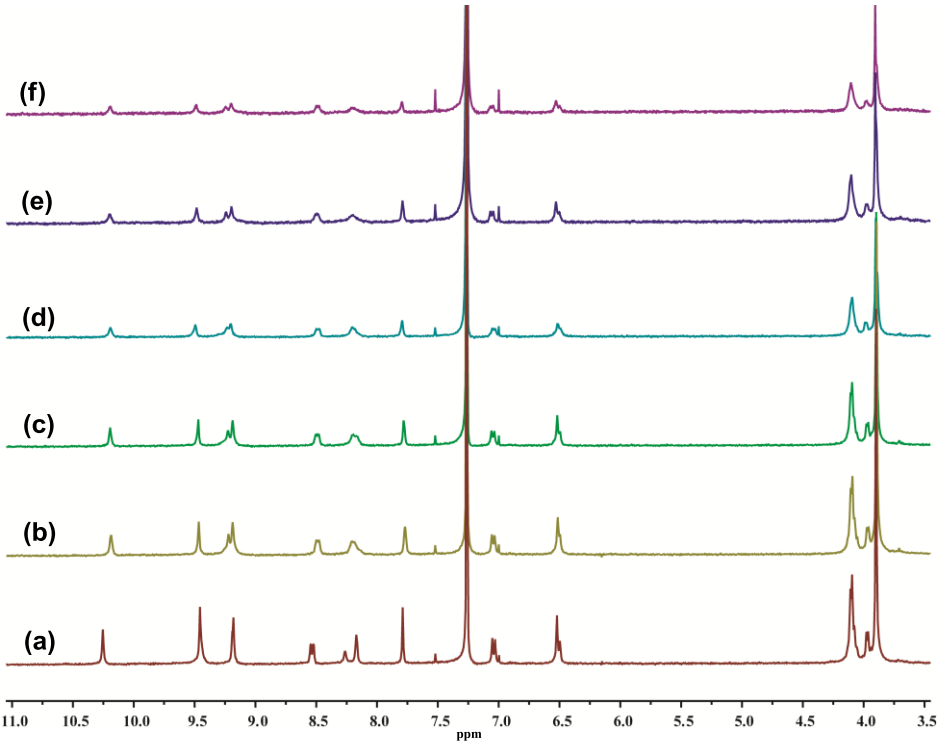

Figure S10. Stacked partial ^{1}H NMR spectra (400 MHz, $CDCl_3$, 298 K) of **2a** at 2.0 mM (a), 1.5 mM (b), 1.0 mM (c), 0.7 mM (d), 0.5 mM (e) and 0.3 mM (f).

5. HR ESI-MS for complex

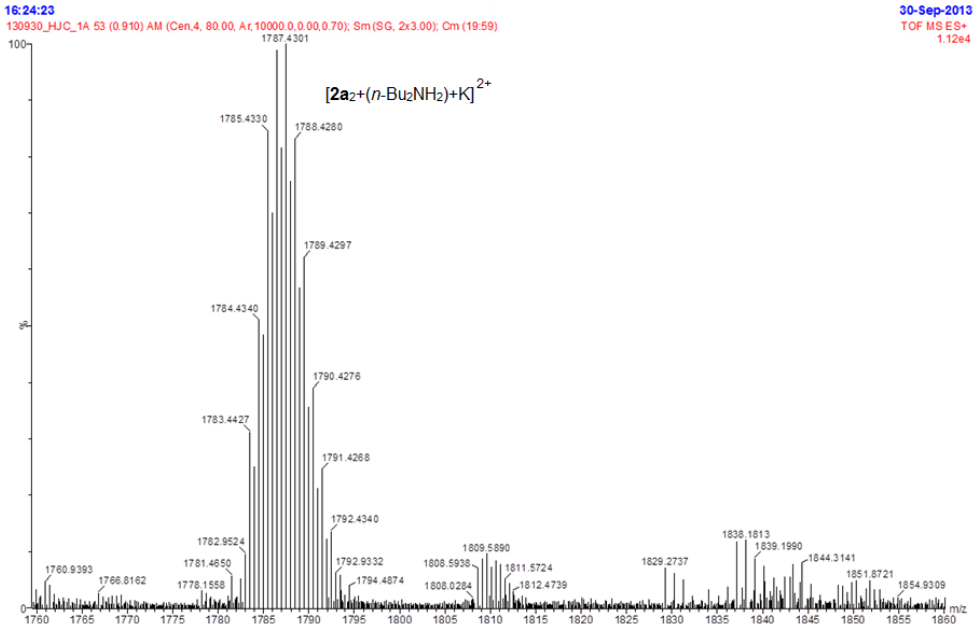

Figure S11. The HRESI MS spectrum of an equimolar solution of **2a** and **G1** in methanol in the positive ion mode.

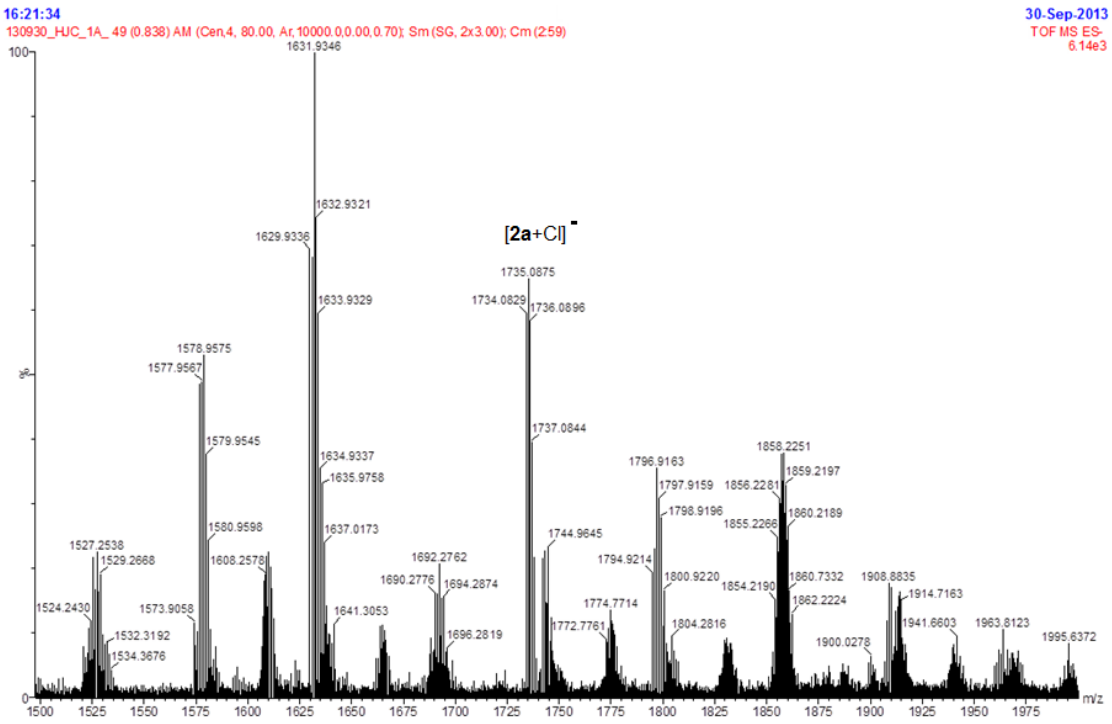

Figure S12. The HRESI MS spectrum of an equimolar solution of **2a** and **G1** in methanol in the negative ion mode.

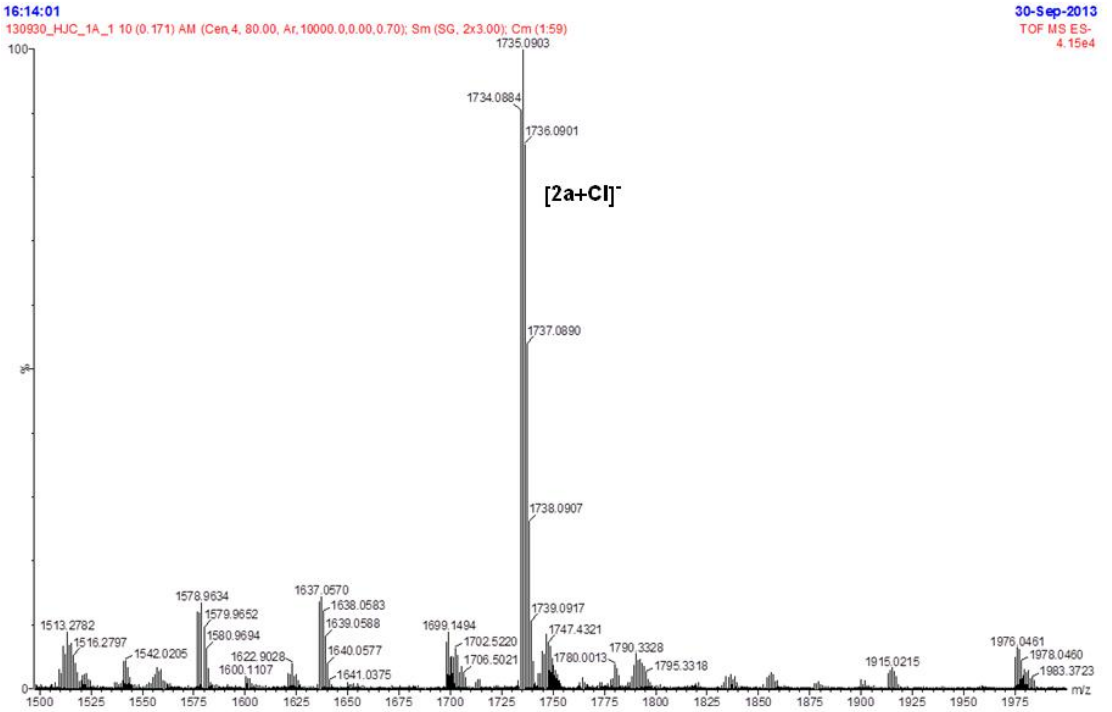

Figure S13. The HRESI MS spectrum of an equimolar solution of **2a** and TBACl in methanol in the negative ion mode.

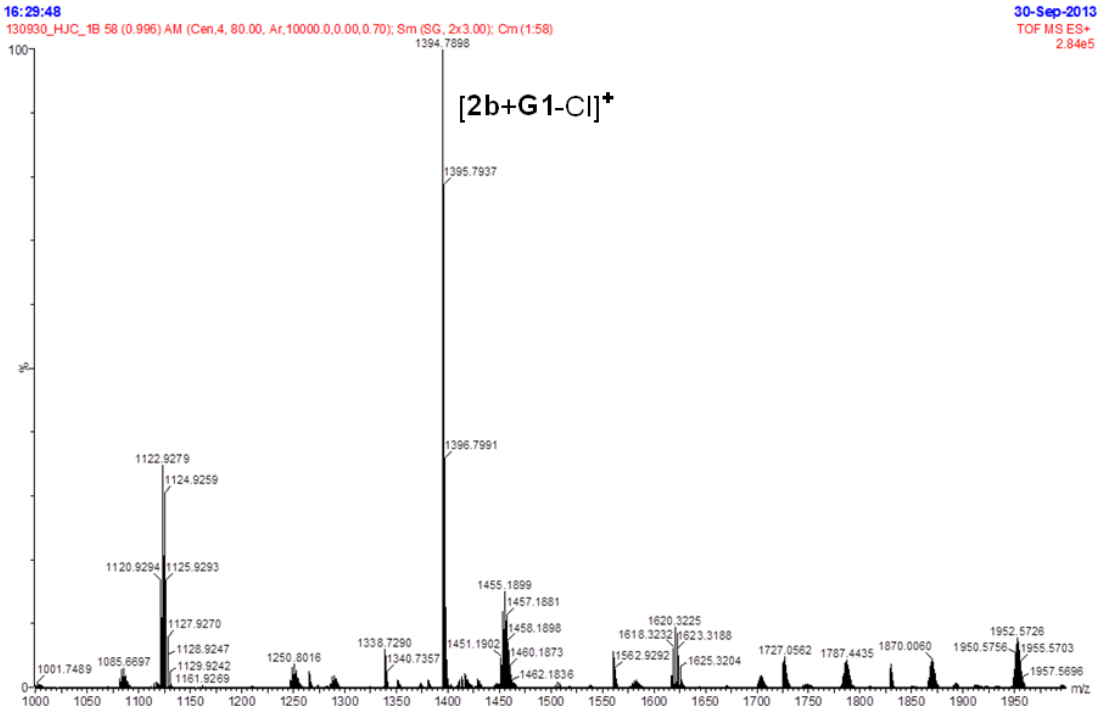

Figure S14. The HRESI MS spectrum of an equimolar solution of **2b** and **G1** in methanol in the positive ion mode.

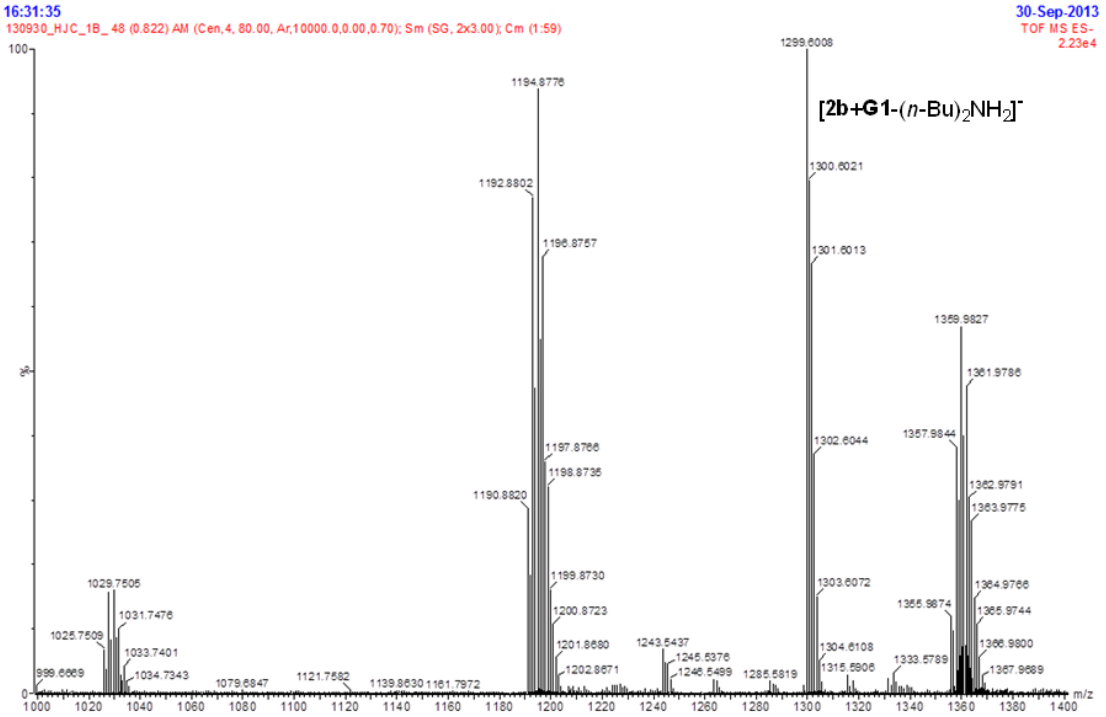

Figure S15. The HRESI MS spectrum of an equimolar solution of **2b** and **G1** in methanol in the negative ion mode.

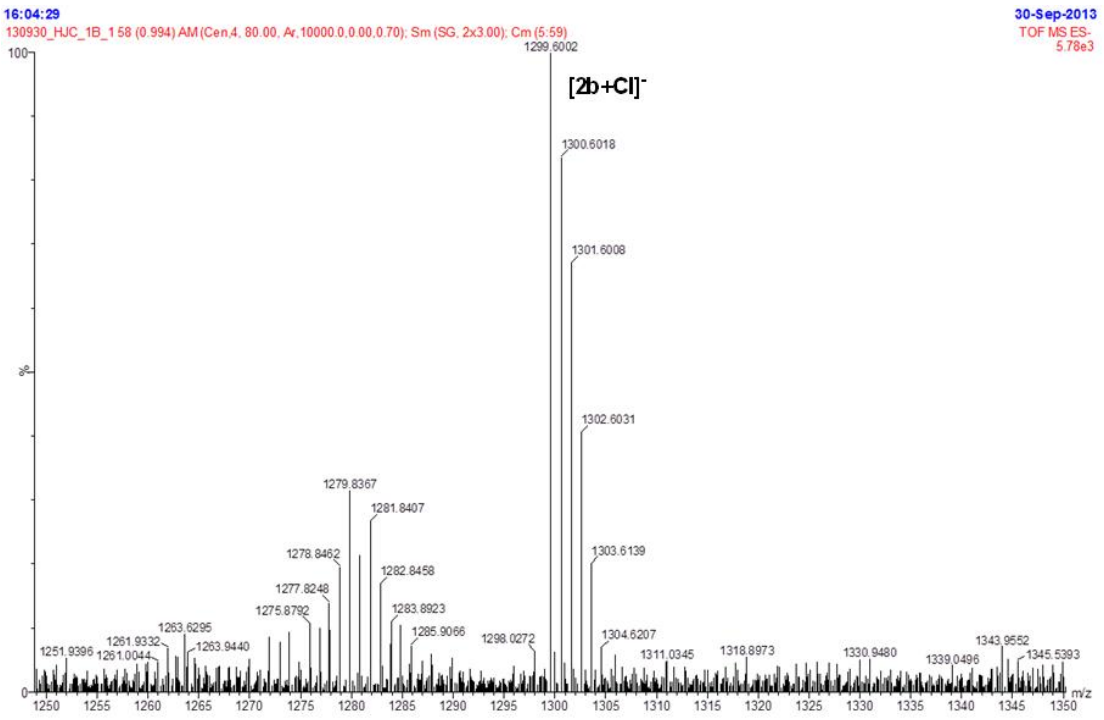

Figure S16. The HRESI MS spectrum of an equimolar solution of **2b** and TBACl in methanol in the negative ion mode.

6. 2D ROESY spectra

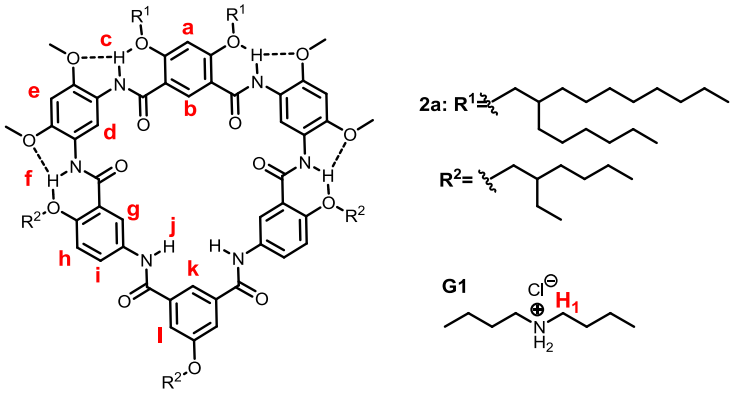

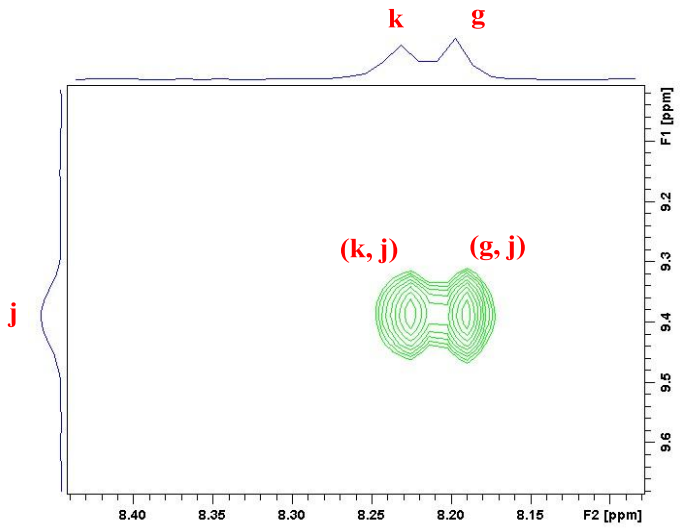

Figure S17. Expanded 2D ROESY spectra of **2a** (10 mM, **2a**:**G1**=1:1) ($CDCl_3$, 400 MHz, 298 K).

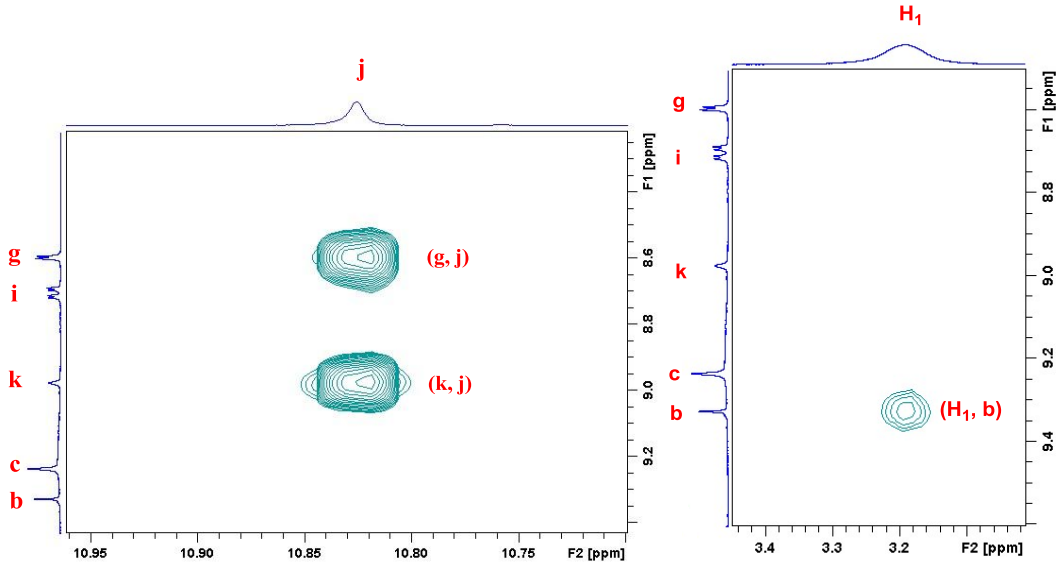

Figure S18. Expanded 2D ROESY spectra of **2a** and **G1** (10 mM, **2a**:**G1**=1:1) ($CDCl_3$, 400 MHz, 298 K).

7. Host-guest complexation of **2a** and **G1**

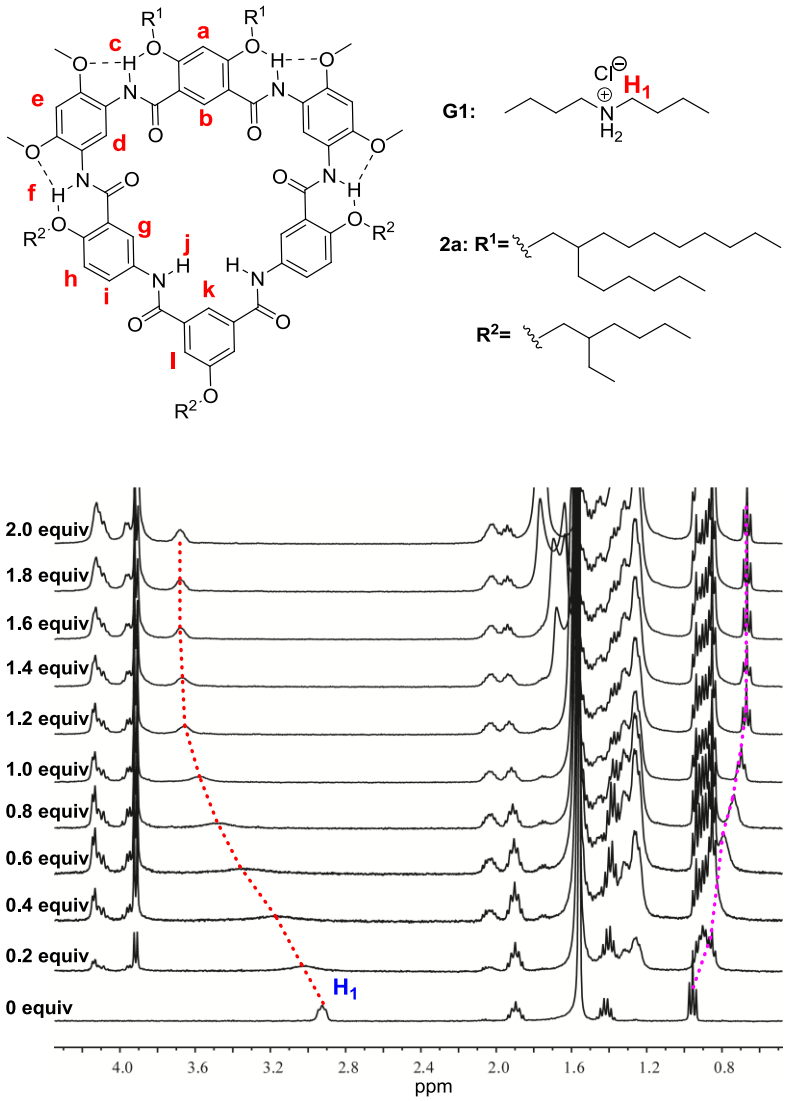

Figure S19. Stacked plots of ^{1}H NMR spectra of compound **G1** (1.0 mM) with cyclo[6]aramide **2a** at different concentration in $CDCl_3$ (400MHz, 298K).

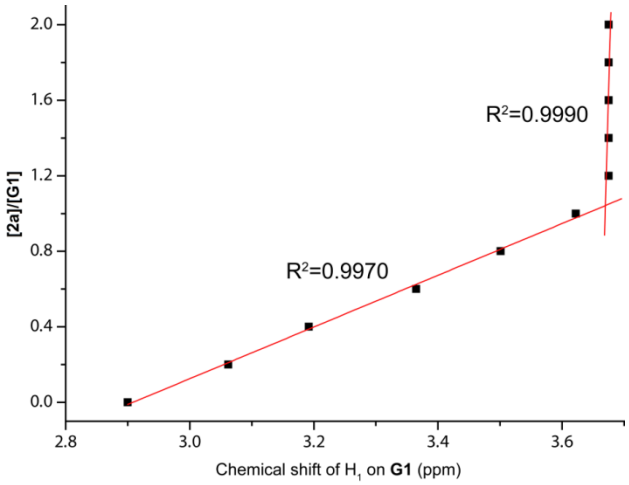

Figure S20. Mole ratio plot for the complexation between **2a** and **G1**, indicating a 1:1 stoichiometry.

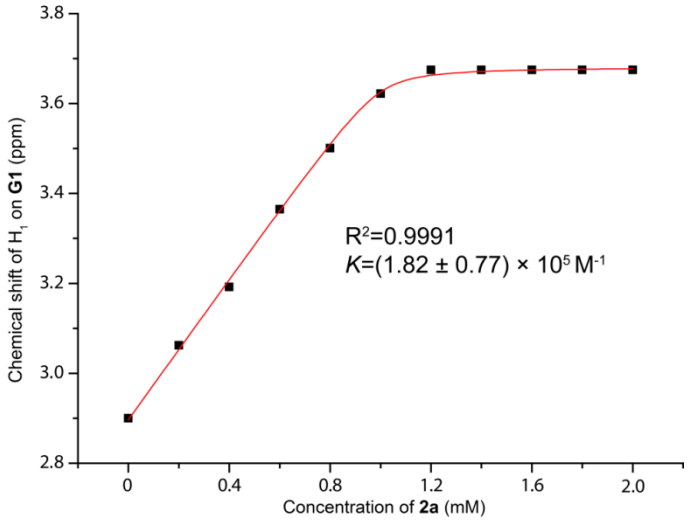

Figure S21. Determination of the binding constant of **2a G1** in $CDCl_3$ at 298 K. Fitting result based on H_1 of compound **G1**.

Table S1. The chemical shifts δ (ppm) for the 1:1 solution of **2a** and **G1** in $CDCl_3$.

Protons	**2a**	**2a+G1**	
	δ_f	δ_b	$\Delta\delta=\delta_b-\delta_f$
H_b	9.18	9.32	0.14
H_c	9.18	9.23	0.05
H_d	9.45	9.63	0.18
H_f	10.25	10.42	0.17
H_g	8.17	8.58	0.41
H_i	8.53	8.70	0.17
H_j	9.18	10.82	1.64
H_k	8.26	8.96	0.70

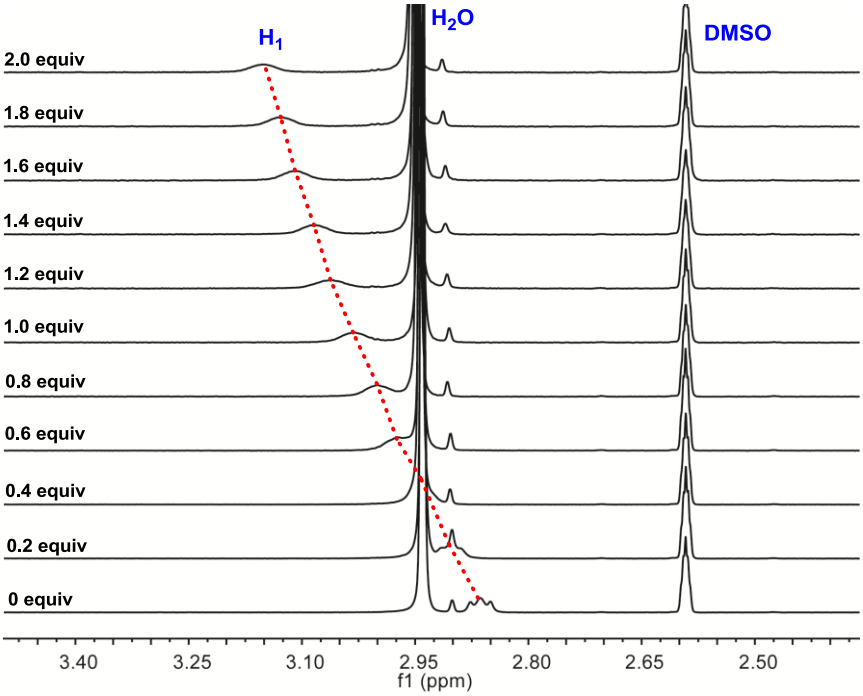

Figure S22. Stacked plots of ^{1}H NMR spectra of compound **G1** (1.0 mM) with cyclo[6]aramide **2a** at different concentration in $CDCl_3$/DMSO-d_6 (v/v = 17:3)(400MHz, 298K).

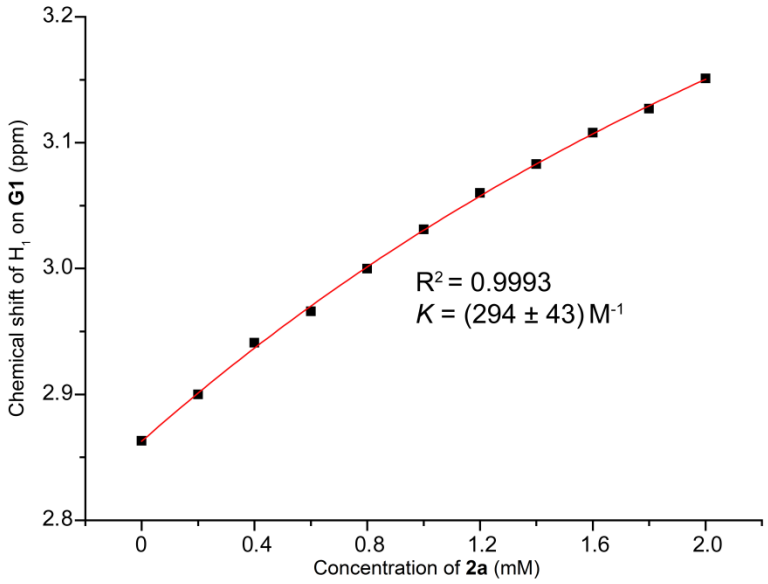

Figure S23. Determination of the binding constant of **2a G1** in $CDCl_3$/DMSO-d_6 (v/v = 17:3) at 298 K. Fitting result based on H_1 of compound **G1**.

8. Host-guest complexation of **2a** and **G2**

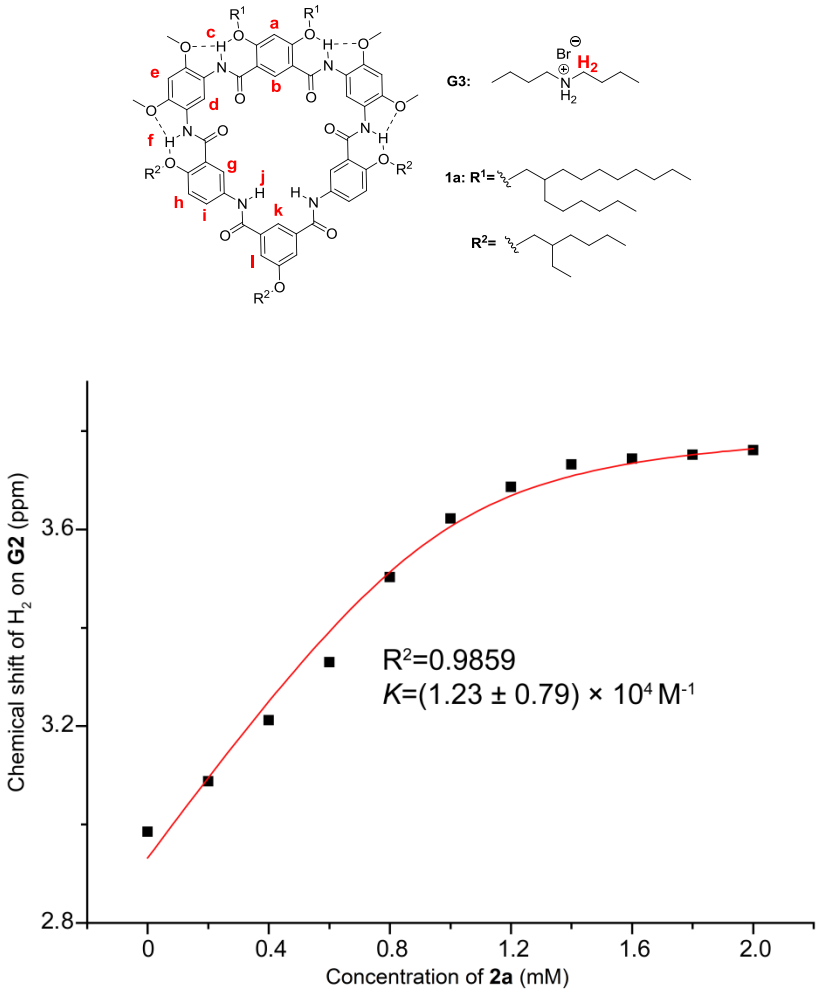

Figure S24. Determination of the binding constant of **2a G2** in $CDCl_3$ at 298 K. Fitting result based on H_2 of compound **G2**.

9. Host-guest complexation of **2a** and **G3**

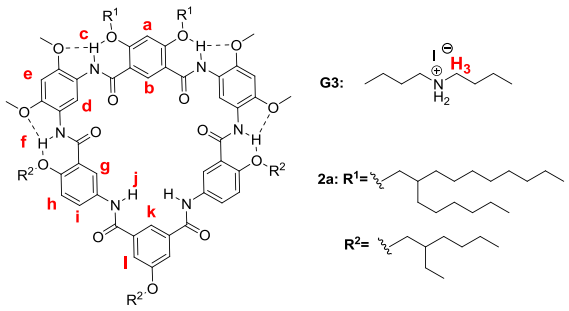

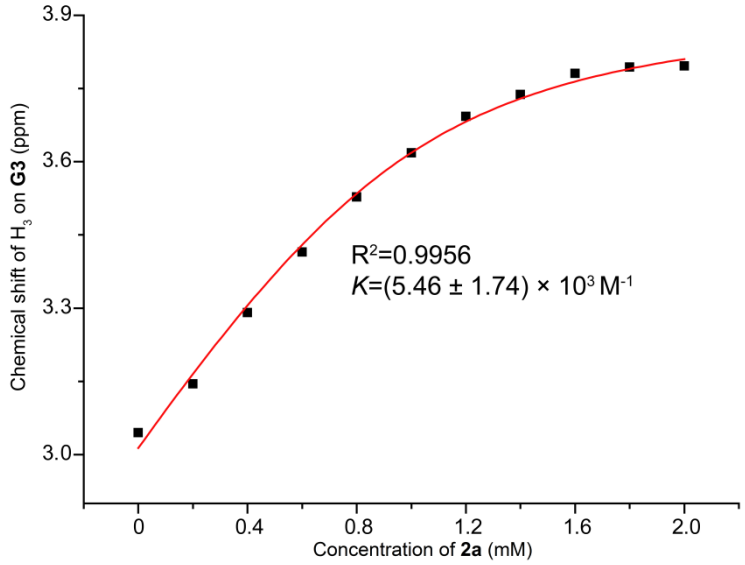

Figure S25. Determination of the binding constant of **2a G3** in $CDCl_3$ at 298 K. Fitting result based on H_3 of compound **G3**.

10. Host-guest complexation of **2a** and **G4**

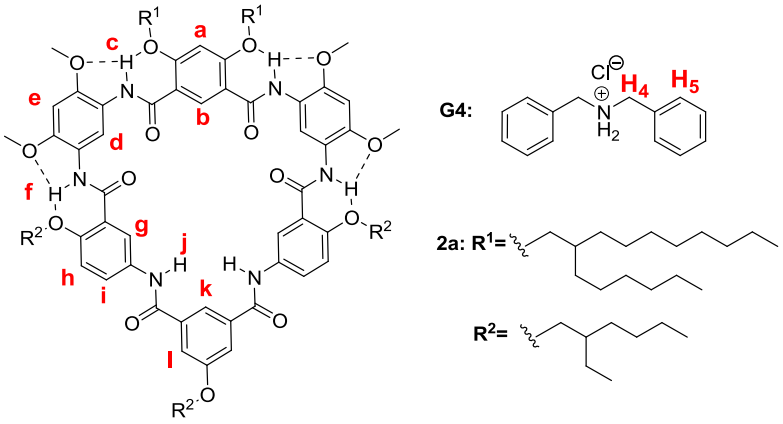

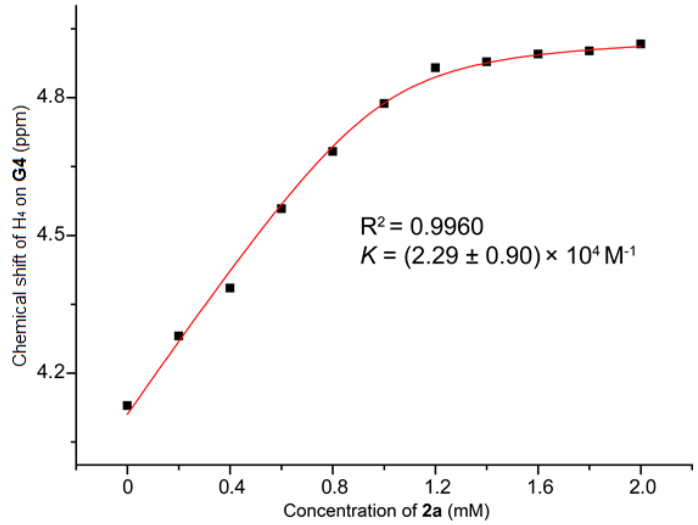

Figure S26. Determination of the binding constant of **2a G4** in $CDCl_3/CD_3CN$ (v/v = 3:2) at 298 K. Fitting result based on H_4 of compound **G4**.

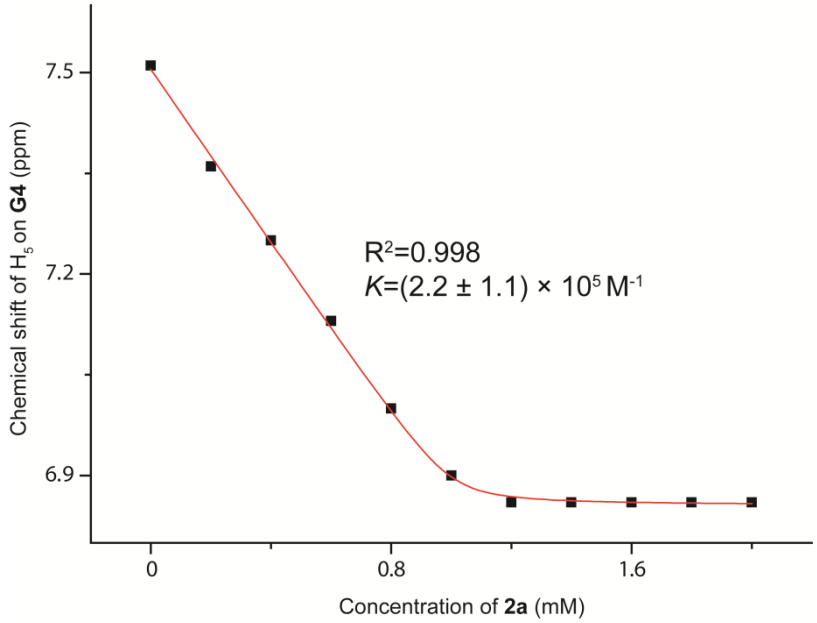

Figure S27. Determination of the binding constant of **2a G4** in $CDCl_3$ at 298 K. Fitting result based on H_5 of compound **G4**.

Table S2. Association constants (K_a/M^{-1})[a] for complexation of host **2a** and guest (**G1**, **G2**, **G3** and **G4**) at 298 K.

Guest	Solvent	**2a**
G1	$CDCl_3$	$(1.8 \pm 0.8) \times 10^5$
G1	$CDCl_3$/DMSO-d_6 (17:3, v/v)	$(2.9 \pm 0.4) \times 10^2$
G2	$CDCl_3$	$(1.2 \pm 0.8) \times 10^4$
G3	$CDCl_3$	$(5.5 \pm 1.7) \times 10^3$
G4	$CDCl_3$	$(2.2 \pm 1.1) \times 10^5$
G4	$CD_3CN/CDCl_3$ (2:3, v/v)	$(2.3 \pm 0.9) \times 10^4$

[a] The association constant K_a values were obtained by ^1H NMR titration.

11. Host-guest complexation of **1** and **G1**

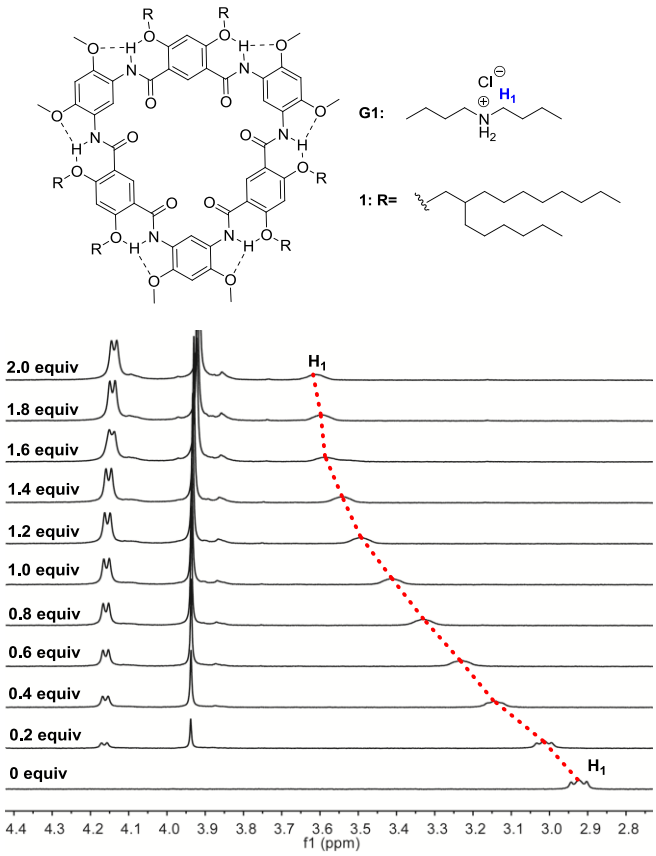

Figure S28. Stacked plots of ^{1}H NMR spectra of compound **G1** (1.0 mM) with cyclo[6]aramide **1** at different concentration in $CDCl_3$ (400MHz, 298K).

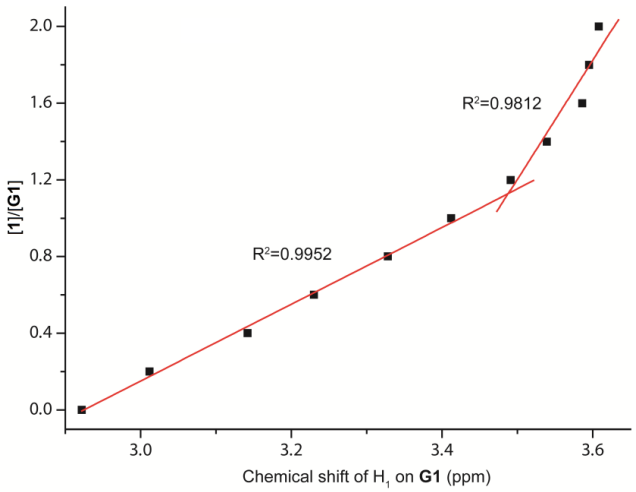

Figure S29. Mole ratio plot for the complexation between **1** and **G1**, indicating a 1:1 stoichiometry.

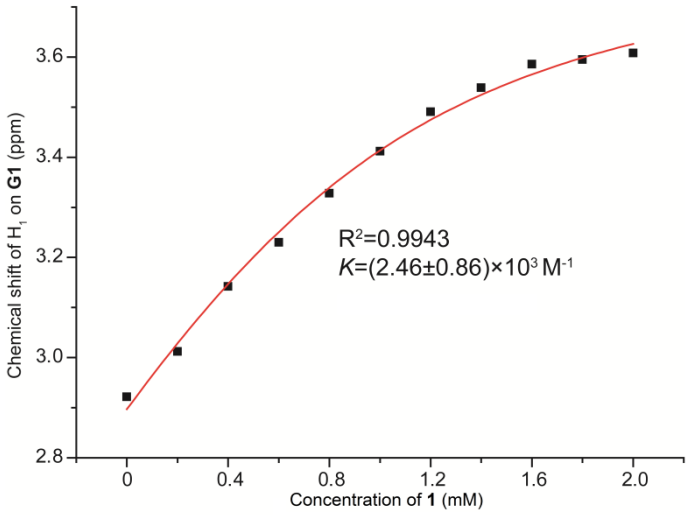

Figure S30. Determination of the binding constant of **1** **G1** in $CDCl_3$ at 298 K. Fitting result based on H_1 of compound **G1**.

12. X-ray single crystal structures of **2b** and [2]pseudorotaxane **2b** **G1**

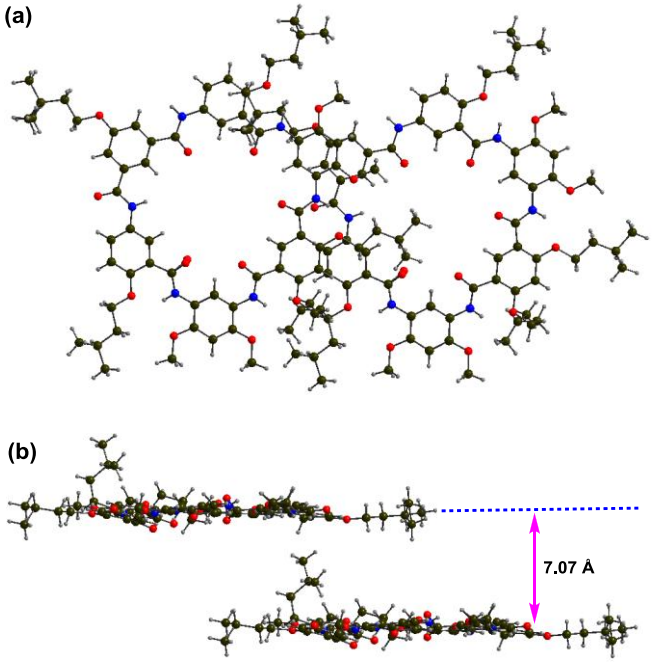

Figure S31. Section of the crystal packing of **2b**: (a) top and (b) side views.

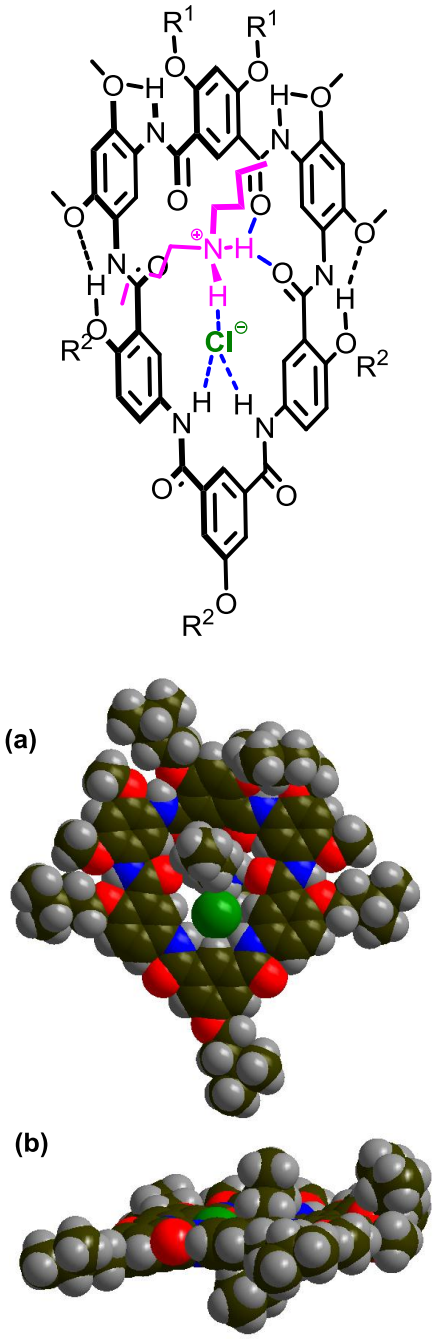

Figure S32. Space-filling packing of the solid-state structure for [2]pseudorotaxane **2b**⊂**G1**: (a) top and (b) side views.

Table S3. Crystallographic data for macrocycle **2b** and [2]pseudorotaxane **2b ⊂G1**

Identification code	**2b**	**2b ⊂G1**
CCDC	976842	976751
Empirical formula	$C_{71}H_{88}N_6O_{15}$	$C_{81}H_{114}Cl_5N_7O_{16}$
Formula weight	1265.47	1619.04
Temperature/K	143.00(10)	143.00(10)
Crystal system	triclinic	monoclinic
Space group	P-1	$P2_1/n$
a/Å	15.0617(6)	15.3283(4)
b/Å	15.8532(5)	24.6571(4)
c/Å	20.3366(6)	23.0091(5)
α/°	86.099(3)	90
β/°	78.810(3)	107.044(2)
γ/°	67.459(4)	90
Volume/Å^3	4399.6(3)	8314.4(3)
Z	2	4
ρ_{calc}mg/mm^3	0.955	1.293
μ(Mo Kα) /mm^{-1}	0.067	0.243
F(000)	1352.0	3448.0
Crystal size/mm^3	0.40 × 0.35 × 0.20	0.3 × 0.3 × 0.2
2Θ range for data collection	5.8 to 52.74 °	5.796 to 52.744 °
Index ranges	-18 ≤ h ≤ 16, -19 ≤ k ≤ 19, -25 ≤ l ≤ 25	-16 ≤ h ≤ 19, -18 ≤ k ≤ 30, -24 ≤ l ≤ 28
Reflections collected	36605	35769
Independent reflections	17942[R(int) = 0.0290]	16968[R(int) = 0.0212]
Data/restraints/parameters	17942/2/852	16968/0/1001
Goodness-of-fit on F^2	0.946	1.067
Final R indexes [I>=2σ (I)]	R^1 = 0.0848, wR^2 = 0.2359	R^1 = 0.0672, wR^2 = 0.1722
Final R indexes [all data]	R^1 = 0.1306, wR^2 = 0.2638	R^1 = 0.0905, wR^2 = 0.1869
Largest diff. peak/hole / e Å^{-3}	1.43/-0.40	1.30/-1.35

13. General description of *ab initio* molecular modeling

All the calculations were carried out by utilizing the Gaussian 09 program package.[4] The geometry optimizations were performed at the density functional theory (DFT) level, and the Becke's three parameter hybrid functional with the Lee-Yang-Parr correlation functional (B3LYP)[5] method was employed to do the calculations. The 6-31G(d,p)[6] basic from the Gaussian basis set library has been used in all the structural optimizations. The harmonic vibrational frequencies and

zero-point energy corrections were calculated at the same level of theory. Single point energy were obtained at the B3LYP level in conjunction with the 6-311+G (2d, p) basis set with the use of the above optimized geometries, i.e., B3LYP/6-311+G(2d,p)//B3LYP/6-31G(d,p). Number of imaginary frequencies is zero.

14. References

1. Gao, R. Z.; Hu, J. C.; Zhang, K.; He, Y. Z.; Liu, P.; Luo, S. Z.; Yang, Y. Q.; Yang, L.; Feng, W.; Yuan, L. H. *Chinese J. Chem.* **2013**, *31*, 689.

2. Li, X. H.; Fang, Y. Y.; Deng, P. C.; Hu, J. C.; Li, T.; Feng, W.; Yuan, L. H. *Org. Lett.* **2011**, *13*, 4628.

3. Kidd, T. J.; Leigh, D. A.; Wilson, A. J. *J. Am. Chem. Soc.* **1999**, *121*, 1599.

4. Frisch, M. J.; Trucks, G. W.; Schlegel, H. B.; Scuseria, G. E.; Robb, M. A.; Cheeseman, J. R.; Scalmani, G.; Barone, V.; Mennucci, B.; Petersson, G. A.; Nakatsuji, H.; Caricato, M.; Li, X.; Hratchian, H. P.; Izmaylov, A. F.; Bloino, J.; Zheng, G.; Sonnenberg, J. L.; Hada, M.; Ehara, M.; Toyota, K.; Fukuda, R.; Hasegawa, J.; Ishida, M.; Nakajima, T.; Honda, Y.; Kitao, O.; Nakai, H.; Vreven, T.; Montgomery, J. A.; Peralta, Jr., J. E.; Ogliaro, F.; Bearpark, M.; Heyd, J. J.; Brothers, E.; Kudin, K. N.; Staroverov, V. N.; Kobayashi, R.; Normand, J.; Raghavachari, K.; Rendell, A.; Burant, J. C.; Iyengar, S. S.; Tomasi, J.; Cossi, M.; Rega, N.; Millam, J. M.; Klene, M.; Knox, J. E.; Cross, J. B.; Bakken, V.; Adamo, C.; Jaramillo, J.; Gomperts, R.; Stratmann, R. E.; Yazyev, O.; Austin, A. J.; Cammi, R.; Pomelli, C.; Ochterski, J. W.; Martin, R. L.; Morokuma, K.; Zakrzewski, V. G.; Voth, G. A.; Salvador, P.; Dannenberg, J. J.; Dapprich, S.; Daniels, A. D.; Farkas, O.; Foresman, J. B.; Ortiz, J. V.; Cioslowski, J.; Fox, D. J. Gaussian, Inc., Wallingford CT, 2009.

5. A. D. Becke, *J. Chem. Phys.*, 1993, **98**, 5648.

6. (a) G. A. Petersson, M. A. Al-Laham, *J. Chem. Phys.*, 1991, **94**, 6081; (b) G. A. Petersson, A. Bennett, T. G. Tensfeldt, M. A. Al-Laham, W. A. Shirley and J. Mantzaris, *J. Chem. Phys.*, 1988, **89**, 2193.